## ▪ SUPPLEMENTARY MATERIAL ▪

# APPENDIX I: METHODS

### Participants and data acquisition

Sixteen healthy right-handed participants (10 males, 6 females) were involved in the study and had no history of psychiatric or neurological disease. The mean (SD) age was 16.9 (1.2) years (range, 15-18 years). All participants gave their written informed consent. This study was approved by the institutional review board of the Seoul National University Hospital.

Imaging was performed using a 1.5-Tesla whole-body scanner (Siemens AVANTO, Germany). Functional images were acquired using an T2*-weighted gradient echoplanar imaging sequence (echo time=52 ms; volume repetition time [TR]=2.34 s; flip angle=90°; in-plane resolution 3.28 × 3.28 mm; slice thickness 5 mm; field of view=210 mm; 64 × 64 matrix; and 25 axial slices).

### Task paradigm

The stimuli consisted of 20 gray-scale pictures of faces (10 Korean male and female faces), with a size of 3.99 × 4.87 cm. They could appear in 35 different positions on the screen. To maintain the degrees of difficulty across the two tasks (face-matching and location-matching) equivalently, only 5 to 9 different faces and 7 different locations were used within each block of each task. The stimuli were back-projected onto a translucent screen placed at the foot of the participant and viewed at a distance of approximately 15 cm from the participant's eyes through mirrors positioned on top of the head coil.

The participants performed a block-designed task in which the face stimuli were used for both the face-matching and location-matching tasks (Supplementary Figure 1). Each task had four experimental conditions: 0-, 1-, 2-, and 3-back. The 0-back condition was the control task, in which participants were asked to press a response button when a face surrounded by a white circle was presented (in the face-matching task) or when a face was displayed at the center of the screen (in the location-matching task). In the n-back face-matching working memory task, the participants were instructed to respond if the presented face was the same as the one presented immediately previously, or two or three faces back. Similarly, in the n-back spatial working memory task, the participants were asked to respond if the face stimulus was in the same place as the position of a face presented in a previous scan, regardless of the identity of the face.

At the beginning of each block, the participants were cued for 2,340 ms regarding which task was to be performed. Each face stimulus was presented for 1,500 ms, followed by 840 ms of fixation. Each task consisted of four sessions. One session consisted of 12 blocks, each of which contained 10 trials (23.4 s). Each of the four working memory load conditions (0-, 1-, 2-, and 3-back) for face and location consisted of six blocks. The interblock interval was 4TR (i.e., 9,360 ms). Behavioral performance during scanning was monitored in terms of reaction time and accuracy. All participants were given a practice task before scanning.

### Preprocessing of functional data

A functional imaging analysis was performed using the Statistical Parametric Mapping 2 (SPM2) software package (http://www.fil.ion.ucl.ac.uk/spm). The first five scans in each run were discarded to eliminate the nonequilibrium effects of magnetization. For each participant, a set of 736 functional scans was realigned to correct for interscan movement and was normalized stereotactically using "Sinc" interpolation into the standard space, defined by the Montreal Neurological Institute (MNI) template. Normalization was performed into the MNI echo planar imaging template. A co-registration process was not executed. The scans were then smoothed using a Gaussian kernel of 8 mm full width at half maximum. Low-frequency signal drift was removed using a 430-s high-pass filter, and temporal autocorrelation in the fMRI time series was corrected using a first-order autoregressive model.

### Activation map

Activation maps were generated for all levels of difficulty and contrasted with the control tasks using a general linear model. Thus, the activated regions presented high BOLD signals in the three difficulty levels relative to that of the control condition. Significance was set at $p<0.0001$ in SPM2, as in the study of Honey et al.,[S1] and the "display slices" procedure (http://imaging.mrc-cbu.cam.ac.uk/imaging/DisplaySlices) was used to display the activation map. Axial images were displayed from z=-4 to 44, with 4-mm increments in the MNI coordinates. We also produced activation maps for each face-matching 1- and 2-back task.

### One-way ANOVA

We performed one-way ANOVA of sixteen subjects with six conditions. T contrast was used for face 1-back task activation con-

trasted with location 1-back task. Face 3-back image contrasted with face 1-back was obtained. Also, location 3-back map contrasted with location 1-back was calculated. Family wise error (FWE) correction was used with p value less than 0.05. A cluster size was larger than 10 voxels.

### Extraction of a time series from each ROI

Based on our activation maps and previous reports, we identified frontoparietal ROIs, including the right and left MFG, the right and left IFG, the medial frontal gyrus, the left SPL, and the right IPL. In the location-matching task, the right insula was selected instead of the right IFG. The threshold of significance was set at $p<0.0001$, and a search for local maxima was performed with SPM2 for each region cluster to identify the coordinates. Each region was labeled using the Talairach Daemon (http://www.talairach.org/). The transformation from MNI to Talairach coordinates was performed using the mni2tal function in the MATLAB software platform. The coordinates for the location-task-related regions were obtained using the same method, with one modification: the left MFG was selected at $p<0.0005$ for all difficulty levels because this region was not clearly defined on the $p<0.0001$ activation map.

MarsBar (http://marsbar.sourceforge.net) was used to extract the time series of the mean values for each ROI.[S2] Each ROI was defined using a sphere with a radius of 4 mm. The union ROI was then obtained from the face and location ROIs with a 4-mm radius for each sphere.[S3] The time series of the mean values for each ROI was extracted from the union ROI using the default option in MarsBar.

### SEM

Session specific linear detrending was performed first to correct for scanner drift. Then blocks of the same type of task were extracted with a one-scan delay to correct for hemodynamic delay.[S1] Extracted blocks of the same type of task were concatenated. After the concatenation, the time series of each subject were normalized with their mean and SD values. During these procedures, the task-"unrelated" signal changes were discarded while keeping all task-related data. Task-related temporal activation was extracted for each region using principal component analysis (PCA).[S1,S4,S5] PCA calculates the eigenvalues and eigenvectors for each task, and the resulting eigenseries (i.e., the specific time series) corresponding to the largest eigenvalue is the task-related time series for each region.[S4]

We used AMOS 7.0 (SPSS Inc., Chicago, IL, USA; http://www.spss.com/Amos/) to construct an effective connectivity diagram based on a maximum-likelihood (ML) algorithm, which identifies the model covariance that minimizes the discrepancy function. The discrepancy function (F) is a form of the log ML function, $F=\log|\Sigma|+\mathrm{tr}(S\Sigma^{-1})-\log|S|-k$, where $\Sigma$ is the model covariance, S is the sample covariance, tr denotes the trace of a matrix, and k is the number of variables (or brain regions).[S4,S5] Model covariance was obtained with the Gaussian noise and a path model matrix. The path model matrix describes the causal relations between source and target regions in the model. Exact formulae for SEM are presented in Bullmore et al.[S4] Each node of a region was assumed to be an exogenous variable with single-headed arrows pointing to it. Each exogenous node was accompanied by an error node (i.e., a residual node with a unit regression coefficient).[S6]

Goodness-of-fit index (GFI) correlates with a reduction in the value of the discrepancy function of a model relative to the value of the discrepancy function with no connection. A high GFI indicates a large reduction in the discrepancy function during optimization. Root mean square error of approximation (RMSEA) is the root mean square of the minimized value of the discrepancy function of the population, divided by degree of freedom (DF), and reflects the compensation for the effect of model complexity. DF increases as the model becomes simpler, and RMSEA thus decreases under this condition. Time series data are not independent and the goodness of fit estimates may be biased. Therefore, goodness-of-fit measures and p-value in model fitting just show how well does the model fit.

### Model generation

First, the right MFG → right IFG and the right IFG → right IPL connections were assumed and drawn in AMOS workspace. This assumption is based on the hypothesis that imagery rehearsal consists of image generation instructions from the MFG to the IFG, followed by the transportation of the created image to the IPL buffer. This hypothesis in turn is based on the sketchpad concept.[S7] The flow of the instruction and generated image is analogous to the top-down flow of verbal information through the articulatory rehearsal in the left hemisphere.[S1,S4] We used the automated search method to construct the model.[S1,S4] In the automated search method, we endowed the model with a directional connection to the ROI concerned, which was identified as that with the largest modification index. After incorporating causation into the model, we reassessed the largest modification index. The above procedure was repeated until the modification decreased under the threshold.

The causal connection of the maximum modification index indicates the steepest direction of the discrepancy function that is to be minimized in the optimization of the log likelihood.[S4] When no additional paths were suggested by the modification index of AMOS (the modification index threshold was set at 4), we generated a symmetric model diagram, excluding the arrows between two similar regions that had a reciprocal direction. This rule stems from the recurrent network feature of the SEM method,[S4] which has no reciprocal feedback loops. The face-matching 1-back task was used to generate the model of a face task. The face-matching 2- and 3-back data were within reasonable statistical limits (i.e., GFI> 0.9, RMSEA<0.1, and p>0.05).

A similar method was used for the location-matching task. The location 1-back model was not statistically valid for the location 2- and 3-back task data. However, the location 2-back model satisfied the criteria for the location 1- and 2-back task data, whereas the location 3-back task data failed to satisfy the criteria. Therefore, the location 2-back task was used to generate the location-matching task model.

## APPENDIX II: INDIVIDUAL SEM

We performed the individual SEM analysis for 16 subjects to examine and avoid the possibility of biased goodness of fit estimates in the SEM analysis. Session specific detrending was performed. Blocks of one condition were then concatenated for each seven ROIs. Normalization of the concatenated time series with mean and SD was done. AMOS software was used for each subject's normalized time series with the models described in the model generation section of Methods. Path coefficients were obtained and their mean and SD values were calculated over sixteen subjects.

Supplementary Table 3 shows the mean path coefficient and SD values over sixteen subjects. Mean path coefficients of right MFG → right IPL over face 1-, 2-, and 3-back tasks were 0.376, 0.347, and 0.360. Mean values of left IFG → left SPL for three face tasks were 0.055, 0.219, and 0.150. Mean path coefficients of right MFG → left SPL for location 1-, 2-, and 3-back tasks were 0.355, 0.393, and 0.360. Increased path coefficient value of the right MFG → the right IPL was observed in the face 1-back task, suggesting a visual imagery during the task. In addition, mean value of the left IFG → he left IPL was high in face 2-back task, which may indicate involvement of the articulatory rehearsal loop. Overall, the results from individual SEM analysis support the results from the effective connectivity analysis in the previous section. For example, the causal connections of the right MFG → the right IPL and the left IFG → the left SPL are important connections in the face 1-back and 2-back task, respectively. These results were statistically significant in the SEM analysis, and supported by the mean of 16 individual coefficients (Supplementary Table 3).

## APPENDIX III: DYNAMIC CAUSAL MODELING (DCM), SLICE TIMING CORRECTIONS, AND LIMITATIONS OF SEM

### Dynamic causal modeling (DCM), slice timing corrections, and limitations of SEM

On a closing note, we discussed a few possible problems and limitations in our methodology. First, we primarily considered SEM instead of DCM to analyze our data. In fact, DCM is another reasonable approach to explore effective connectivity among different brain regions (e.g. Friston[S8]). However, SEM had additional advantages in analyzing our imaging data compared to DCM. For example, SEM can model interaction at the hemodynamic level while DCM models at neuronal level. SEM also enables to avoid arbitrary postulation of connectivity patterns among different regions.[S9] And it was possible to extract time series containing common major component across the subjects in SEM. PCA was used in this step.

Second, we did not apply slice timing correction to our data. In a block design, several scans are averaged together in data analysis. Averaging several scans can sacrifice gain in accuracy of slice timing. Therefore, applying the slice timing correction procedure is not likely to make any change in our measurement of causality.

Last, there are limitations in our SEM methods: We used a data driven automated search method to build our model, which uses local fit gradients (i.e. modification indices). However, it should be noted that even very different models can have identical fit, and moreover, some parts of the non-recursive model space cannot be explored. In addition, models with lots of loops or bidirectional connections are biologically plausible but not mathematically identifiable with SEM.

### REFERENCES

S1. Honey GD, Fu CH, Kim J, Brammer MJ, Croudace TJ, Suckling J, et al. Effects of verbal working memory load on corticocortical connectivity modeled by path analysis of functional magnetic resonance imaging data. Neuroimage 2002;17:573-582.

S2. de Marco G, de Bonis M, Vrignaud P, Henry-Feugeas MC, Peretti I. Changes in effective connectivity during incidental and intentional perception of fearful

faces. Neuroimage 2006;30:1030-1037.
S3. Koshino H, Kana RK, Keller TA, Cherkassky VL, Minshew N, Just MA. 2008. fMRI investigation of working memory for faces in autism: visual coding and underconnectivity with frontal areas. Cereb Cortex 2008;18:289-300.
S4. Bullmore E, Horwitz B, Honey G, Brammer M, Williams S, Sharma T. How good is good enough in path analysis of fMRI data? Neuroimage 2000;11:289-301.
S5. Kim J, Horwitz B. How well does structural equation modeling reveal abnormal brain anatomical connections? An fMRI simulation study. Neuroimage 2009; 45:1190-1198.
S6. Arbuckle JL. Amos 16.0 User's Guide. Chicago: SPSS Inc; 2007.
S7. Baddeley A. Working memory: looking back and looking forward. Nat Rev Neurosci 2003;4:829-839.
S8. Friston KJ, Harrison L, Penny W. Dynamic causal modeling. Neuroimage 2003;19:1273-1302.
S9. Penny WD, Stephan KE, Mechelli A, Friston KJ. Modelling functional integration: a comparison of structural equation and dynamics causal models. Neuroimage 2004;23(Suppl 1):S264-S274.

**Supplementary Table 1.** One-way ANOVA results

| Area | BA | MNI coordinates | | | Cluster size | t-value |
|---|---|---|---|---|---|---|
| | | x | y | z | | |
| Face 1 vs. Location 1 | | | | | | |
| L OL | 18 | -30 | -96 | -6 | 61 | 7.10 |
| R OL | 18 | 24 | -99 | -6 | 58 | 7.26 |
| Face 3 vs. Face 1 | | | | | | |
| L MFG/SMA | 8 | -3 | 24 | 48 | 17 | 5.60 |
| Location 3 vs. Location 1 | | | | | | |
| L MFG/SMA | 6 | -6 | 24 | 48 | 134 | 7.25 |
| R MFG/SMA | | 6 | 24 | 48 | | 6.33 |
| L MFG | 6 | -27 | 6 | 57 | 34 | 5.02 |
| R MFG | | 27 | 12 | 54 | | 6.62 |
| | | 33 | 6 | 51 | | 6.34 |
| R IPL | 40 | 48 | -45 | 48 | 72 | 6.08 |
| R SPL | 7 | 21 | -63 | 51 | 23 | 5.52 |

ANOVA: analysis of variance, MINI: Mini International Neuropsychiatric Interview, L: left, R: right, BA: brodmann area, OL: occipital lobe, MFG: middle frontal gyrus, SMA: supplementary motor are, IPL: inferior parietal lobule, SPL: superior parietal lobule

**Supplementary Table 2.** Estimated path coefficients and p values for face- and location-matching n-back tasks

| Path connections | 1-back | | 2-back | | 3-back | |
|---|---|---|---|---|---|---|
| | Coefficient | p value | Coefficient | p value | Coefficient | p value |
| Face | | | | | | |
| R MFG → R IFG | 0.038 | 0.767 | 0.151 | 0.236 | 0.046 | 0.717 |
| R MFG → L MFG | 0.344 | 0.006 | 0.322 | 0.009 | 0.127 | 0.328 |
| R IFG → L IFG | 0.343 | 0.006 | 0.555 | <0.001 | -0.169 | 0.181 |
| L MFG → L IFG | 0.073 | 0.554 | 0.051 | 0.636 | -0.268 | 0.030 |
| R IFG → R IPL | 0.008 | 0.945 | -0.167 | 0.203 | 0.149 | 0.233 |
| R MFG → R IPL | 0.390 | 0.001 | 0.014 | 0.911 | 0.115 | 0.347 |
| L MFG → MedFG | 0.265 | 0.043 | -0.246 | 0.064 | -0.005 | 0.972 |
| R MFG → MedFG | 0.129 | 0.330 | -0.012 | 0.926 | -0.026 | 0.839 |
| L MFG → L SPL | 0.040 | 0.760 | -0.129 | 0.295 | -0.063 | 0.630 |
| L IFG → L SPL | -0.001 | 0.997 | 0.336 | 0.006 | 0.172 | 0.190 |
| Location | | | | | | |
| R MFG → L SPL | 0.084 | 0.525 | 0.382 | 0.002 | 0.088 | 0.504 |
| R MFG → R Insula | 0.129 | 0.322 | 0.023 | 0.859 | 0.410 | <0.001 |
| L SPL → MedFG | -0.019 | 0.883 | 0.292 | 0.020 | 0.305 | 0.010 |
| R Insula → R IPL | -0.179 | 0.160 | 0.044 | 0.724 | 0.124 | 0.290 |
| R Insula → L IFG | 0.597 | <0.001 | 0.467 | <0.001 | 0.469 | <0.001 |
| L SPL → L IFG | 0.087 | 0.408 | 0.263 | 0.016 | 0.019 | 0.872 |
| MedFG → R IPL | -0.093 | 0.464 | 0.275 | 0.027 | 0.427 | <0.001 |
| L MFG → L IFG | 0.100 | 0.348 | -0.061 | 0.573 | 0.199 | 0.084 |
| L MFG → R IPL | 0.042 | 0.746 | 0.035 | 0.778 | 0.079 | 0.492 |

Coefficients with p<0.05 are indicated in bold and represent causations that were significantly different from a null connection. L: left, R: right, MFG: middle frontal gyrus, IFG: inferior frontal gyrus, IPL: inferior parietal lobule, MedFG: medial frontal gyrus, SPL: superior parietal lobule

**Supplementary Table 3.** Mean path coefficient and SD values for face- and location-matching n-back tasks in the individual SEM analysis

| Path connections | 1-back | | 2-back | | 3-back | |
|---|---|---|---|---|---|---|
| | Mean | SD | Mean | SD | Mean | SD |
| Face | | | | | | |
| R MFG → R IFG | 0.432 | 0.280 | 0.359 | 0.280 | 0.495 | 0.139 |
| R MFG → L MFG | 0.465 | 0.197 | 0.524 | 0.184 | 0.514 | 0.175 |
| R IFG → L IFG | 0.537 | 0.190 | 0.543 | 0.168 | 0.538 | 0.134 |
| L MFG → L IFG | 0.179 | 0.154 | 0.151 | 0.123 | 0.216 | 0.136 |
| R IFG → R IPL | 0.025 | 0.409 | 0.130 | 0.193 | 0.166 | 0.165 |
| R MFG → R IPL | 0.376 | 0.159 | 0.347 | 0.154 | 0.360 | 0.172 |
| L MFG → MedFG | 0.292 | 0.183 | 0.187 | 0.252 | 0.288 | 0.209 |
| R MFG → MedFG | 0.192 | 0.195 | 0.303 | 0.182 | 0.278 | 0.208 |
| L MFG → L SPL | 0.343 | 0.171 | 0.320 | 0.152 | 0.350 | 0.165 |
| L IFG → L SPL | 0.055 | 0.189 | 0.219 | 0.233 | 0.150 | 0.188 |
| Location | | | | | | |
| R MFG → L SPL | 0.355 | 0.231 | 0.393 | 0.191 | 0.360 | 0.261 |
| R MFG → R Insula | 0.406 | 0.167 | 0.419 | 0.141 | 0.490 | 0.164 |
| L SPL → MedFG | 0.391 | 0.163 | 0.433 | 0.164 | 0.418 | 0.232 |
| R Insula → R IPL | 0.065 | 0.231 | 0.225 | 0.137 | 0.123 | 0.256 |
| R Insula → L IFG | 0.564 | 0.143 | 0.551 | 0.153 | 0.586 | 0.173 |
| L SPL → L IFG | 0.043 | 0.119 | 0.068 | 0.146 | 0.073 | 0.163 |
| MedFG → R IPL | 0.332 | 0.217 | 0.355 | 0.179 | 0.362 | 0.229 |
| L MFG → L IFG | 0.183 | 0.155 | 0.136 | 0.131 | 0.159 | 0.114 |
| L MFG → R IPL | 0.129 | 0.188 | 0.156 | 0.111 | 0.230 | 0.170 |

L: left, R: righ, MFG: middle frontal gyrus, IFG: inferior frontal gyrus, IPL: inferior parietal lobule, MedFG: medial frontal gyrus, SPL: superior parietal lobule

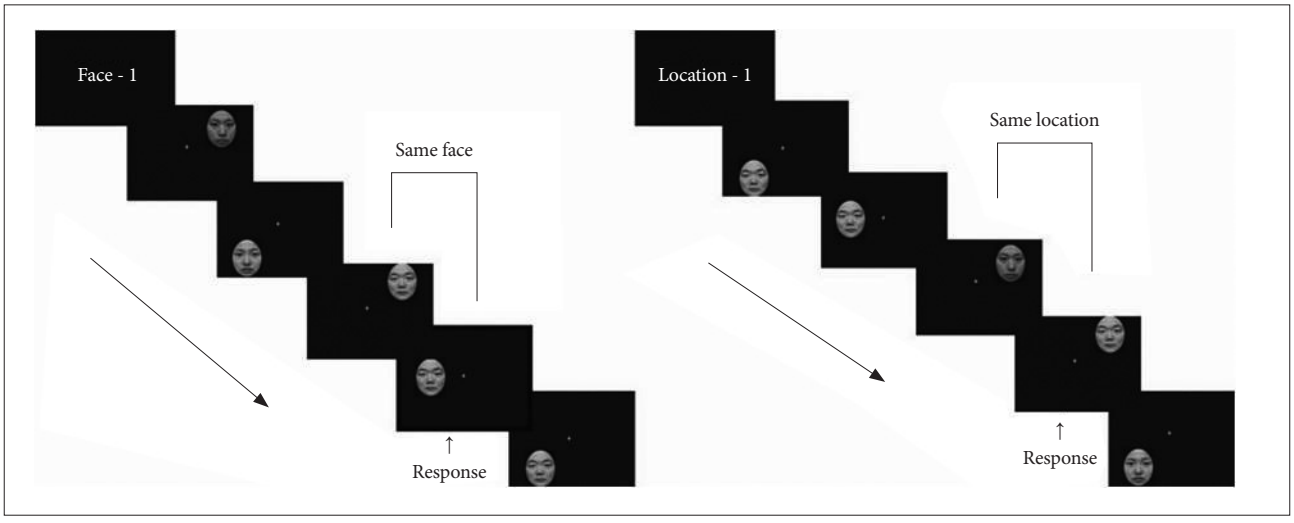


**Supplementary Figure 1.** Face-matching 1-back task (left) and location-matching 1-back task (right). The same face as that shown in the preceding scan appeared in the scan indicated by the arrow in the face-matching 1-back task figure. The same location as that presented in the preceding scan was occupied by the face of the scan indicated by the arrow in the location-matching 1-back task.